Gem-Quality Andalusite from Brazil

Authors: *Shyamala Fernandes and Gagan Choudhary*

(This article was first appeared in Gems & Gemology, Vol. 45, No. 2, pp 120-129)

Introduction

The name *andalusite* is derived from the Andalusia region of southern Spain, where the mineral was first discovered (Dana and Ford, 1992). Gem-quality material is known from Brazil (Espírito Santo and Minas Gerais States), Sri Lanka, the United States, Madagascar, Russia (Siberia), Myanmar (O'Donoghue, 2006), and China (Liu, 2006). Andalusite varieties include highly pleochroic brownish pink/green (e.g., figure 1), Mn-rich bright green ("viridine"), and chiastolite. The last is typically opaque and features a dark cross-shaped pattern formed by carbonaceous inclusions (Webster, 1994; O'Donoghue, 2006).

This article reports the properties recorded from an ~1 kg parcel of medium-quality andalusite that was purchased from a merchant in Jaipur, who deals in rough from Brazil. The exact location in Brazil was, unfortunately, not available.

Figure 1: Brazil is a source of rare gem-quality andalusite, as shown by this stone. Due to its strong pleochroism, both dominating pleochroic colours are distinctly visible.

Materials and Methods

From the parcel of rough, we randomly selected about 150 specimens for examination that ranged from ~0.4 to 3 g. We studied 15 samples in detail for their crystallographic features, surface markings, cleavage directions, and pleochroism with respect to crystallographic orientation. These samples exhibited a variety of colours: green, yellowish green to brownish green, brownish pink, and distinctly bicoloured pink and green. In addition, we selected six samples of the pinkish brown to brownish pink variety chiastolite, which displayed distinct (sometimes partial) cross-shaped arrangements of dark inclusions. About 20% of the 150 specimens were chiastolite, and they ranged in diaphaneity from transparent to opaque.

We selected 72 of the 150 specimens, of moderate commercial quality, for fashioning on the basis of their colouration, clarity, and projected yield. Of these, 18 were faceted (figure 2) and the other 54 were left preformed. The preformed stones were categorized into three colour groups: green (17 specimens), brownish pink (14), and strongly pleochroic pinkish brown/yellowish green (23). On an additional seven specimens (figure 3), we polished the largest parallel surfaces so we could obtain RI readings and examine their internal features.

Figure 2: Eighteen andalusite samples (0.15–0.58 ct) were faceted to display the range of colour

Figure 3: Seven andalusite specimens (0.81–3.87 ct) were polished as slices for inclusion studies and RI readings

Standard gemmological tests--including colour observations, SG measurements, fluorescence reactions, and visible-range spectroscopy--were performed on all samples. RI and optic sign were measured only on the seven polished slices and the 18 faceted samples. To determine the variations in refractive index with respect to crystallographic axis, we polished the prism faces [(110), (1¯1¯0), (11¯0), (1¯10)], one of the corners [representing (100) or (010)], and the pinacoidal face (001) of one prismatic crystal. RI was measured with a GemLED refractometer. We obtained hydrostatic SG values using a Mettler Toledo CB 1503 electronic balance. Fluorescence was tested using standard long-wave (366 nm) and short-wave (254 nm) UV bulbs. Absorption spectra were observed using a desk-model GIA Prism 1000 spectroscope. We examined internal features with both a binocular gemmological microscope and a horizontal microscope with immersion, using fibre-optic and other forms of lighting (including darkfield and brightfield).

Qualitative energy-dispersive X-ray fluorescence (EDXRF) chemical analyses of 31 green and brownish pink preforms, the seven polished slices, and the 18 faceted samples were performed with a PANalytical Minipal 2 instrument using two different conditions. Elements with lower atomic number (e.g., Al and Si) were measured at 4 kV tube voltage and 0.850 mA tube current with no filter; transition and heavier elements were analyzed at 25 kV and 0.025 mA using an Al filter.

Infrared spectra of 31 preforms (green and brownish pink), 15 crystals (4–15 mm thick), seven polished slices, and five faceted samples that had undergone fracture-filling processes were recorded in the 6000–400 cm^{-1} range at a standard resolution of 4 cm^{-1}; 50 scans per sample were recorded with a Nicolet Avatar 360 Fourier-transform infrared (FTIR) spectrometer at room temperature in transmission mode. We collected multiple spectra to find the orientation of best transmission (depending on the thickness and transparency of the samples), considering the pleochroic colours and crystallographic axes.

Raman analysis was performed on five rough samples and two polished slices in two directions—along the c-axis and along the a- or b-axis—in the 2000–100 cm^{-1} range using a Renishaw InVia Raman confocal microspectrometer with 514 nm Ar-ion laser excitation, an exposure time of 10 seconds per scan, and 10 scans per sample.

We selected 24 rough samples for heat-treatment experiments; the original colours were brownish pink (8 samples), green (5), bicoloured (3), and brownish pink with a green component at their corners (8). We heated the stones in a muffle furnace with digital temperature controls. Six stones were heated at 350°C and eight at 550°C for 8 hours, while 10 samples were heated at 800°C for 2½ hours and then at 550°C for 5½ hours.

Of the 18 faceted samples, five with eye-visible surface-reaching fissures were selected for fracture filling. We used a colourless epoxy resin on three samples and Johnson & Johnson baby oil (also colourless) on two samples, at pressures of 40 to 50 psi for 48 hours. The samples were photo-documented before the experiments, and the colours and inclusions were compared before and after the treatments.

Results and Discussion

Crystal Morphology and Visual Observations. The majority of the rough consisted of broken crystals with frosted surfaces. Approximately 10% of them were terminated by pinacoids or pyramids (figure 4) and exhibited four-sided prisms, often with the rectangular- or rhomb-shaped cross section associated with the orthorhombic crystal system (Webster, 1994). Most of these crystals had only one termination and were broken at the other end.

Figure 4: Approximately 10% of the specimens in the rough parcel of andalusite displayed characteristic crystal forms with prism faces terminated by pyramids. The crystal shown here weighs 1 g.

More than 80% of the rough displayed pronounced etching, consistent with their frosted surfaces. This was evident on 12 of the 15 crystals selected for crystallographic study. The etching pattern varied from irregular to square or rectangular in shape (figure 5, left). Many of the samples also exhibited striations on the prism faces, parallel to the c-axis. One of the crystals displayed two sets of striations on the same face (figure 5, right). One set

was oriented along the c-axis, while the other consisted of lateral striations; such patterns indicate twinning or various stages of overgrowth where two sectors/crystals have grown in different directions. Some crystals clearly displayed a smaller attached twinned crystal oriented along or inclined toward the c-axis of the main crystal. In addition, step-like planes indicating cleavage (again, see figure 5, left) were present on the surfaces of all the samples studied; only one cleavage plane was seen in most samples, but in some cases two directions were visible. Both directions were oriented parallel to the prism faces, as reported previously (Phillips and Griffen, 1986).

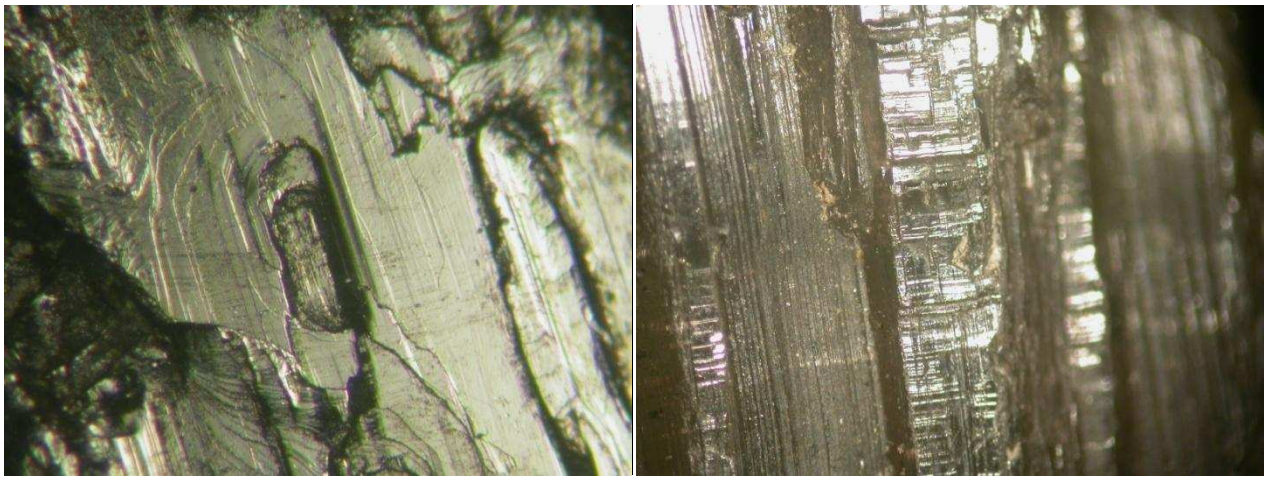

Figure 5: Many of the andalusite samples displayed strong etching that varied from irregular to square or rectangular in shape (left). Also common were striations on the prism faces (right). Note the two-directional striations, one vertical and the other lateral; this indicates the presence of twinning or various stages of overgrowth where two sectors have grown in different directions. Also note the step-like features in the left image, which indicate cleavage planes. Magnified 60x (left) and 45x (right).

About 20% of the pinkish brown/brownish pink samples contained black inclusions that formed partial or complete chiastolite cross patterns. Most of these samples revealed black material in the core when viewed along the c-axis, while a few had a green central core with black outlines and arms. The six specimens selected for study included three with black cores (figure 6) and three with green cores (e.g., figure 7, left). The cores varied from transparent to opaque and from almost square (figure 6, center) to rectangular (figure 6, left and right). The green cores were distinctly pleochroic: When the plane of the core was perpendicular to the viewing angle, it appeared green (again, see figure 7, left); as the host was tilted slightly, the core

appeared brownish pink/red (figure 7, right) while the rest of the stone remained unchanged. A similar effect was visible when the crystals were viewed through prism faces. The colour-zoned or bicoloured green-and-pink samples (figures 8 and 9, left) were similar in appearance to “watermelon” tourmaline.

Figure 6: The chiastolite samples, here ranging from 3 to 6.5 mm thick displayed a characteristic black cross pattern at the basal pinacoid with a square to rectangular core. The unusual transparency of these chiastolites made them particularly interesting.

Figure 7: A small percentage of the brownish pink to pinkish brown andalusite contained a green central core with black outlines and arms. When the plane of the core was perpendicular to the viewing angle, it appeared green (left). As the sample was tilted slightly, it appeared brownish pink to red (right), while the rest of the stone (i.e., the rim) remained unchanged. Magnified 15x

Orientation of Crystal for Best Cut. Overall, the parcel of rough was more suited for beads and cabochons than for faceted stones. Among the major considerations in the cutting process were the abundance of inclusions, bodycolour, and orientation of the pleochroism to achieve the best table-up colour. The brownish pink crystals had about the same colour after cutting (i.e., their strong pleochroism was not visible face up), so the rough was oriented simply for best yield. For the green stones, an attempt was made to orient the green colour to the table; however, crystals that also exhibited a strong pink pleochroic colour displayed a pinkish hue at the corners of the finished stones. Bicoloured stones were specifically cut to display the colour zoning in a table-up position. Crystals with long tube-like inclusions needed to be oriented in such a way that these inclusions were perpendicular to the table facet, to make them less visible. Although the rough sizes ranged from ~0.4 to 3 g, the resulting stones weighed only 0.15–0.58 ct after faceting. The overall yield from rough to the finished product was approximately 20%.

Gemmological Properties. The gemmological properties of the samples are described below and summarized in table 1.

Pleochroism. All but the brownish pink samples displayed strong, eye-visible pleochroism that ranged from weak to strong. Along the c-axis, the samples appeared brownish pink; perpendicular to the c-axis, they appeared yellowish or brownish green. Depending on their orientation and their main bodycolour, the cut stones appeared brownish pink to yellowish green; both colours were often visible in the same sample when viewed table-up (again, see figures 1 and 2). The bicoloured samples also displayed strong pleochroism. In one sample, rotating the polarizer 90° turned the brownish pink area almost colourless while the green portion became brighter yellowish green (see figure 9).

Refractive Index. We recorded a range of RI values--n_α=1.637–1.649 and n_γ =1.646–1.654--with a negative optic sign; birefringence varied from 0.008 to 0.010. These values are consistent with those reported previously for andalusite (Webster, 1994; Phillips and Griffen, 1986). RI and birefringence increase with the increasing percentage of Mn (as in

the viridine variety) to as high as 1.690 with birefringence of about 0.025 (Phillips and Griffen, 1986), although not in our specimens. Measurements of the oriented sample revealed that the pinacoidal face (001), or α-ray direction, gave the lowest RIs and birefringence (0.008), while the polished corner (100) or (010) gave the highest values (with maximum birefringence of 0.009), indicating that it represented the b-axis or γ-ray direction. Such variations were reported previously by Kerr (1959) and Phillips and Griffen (1986).

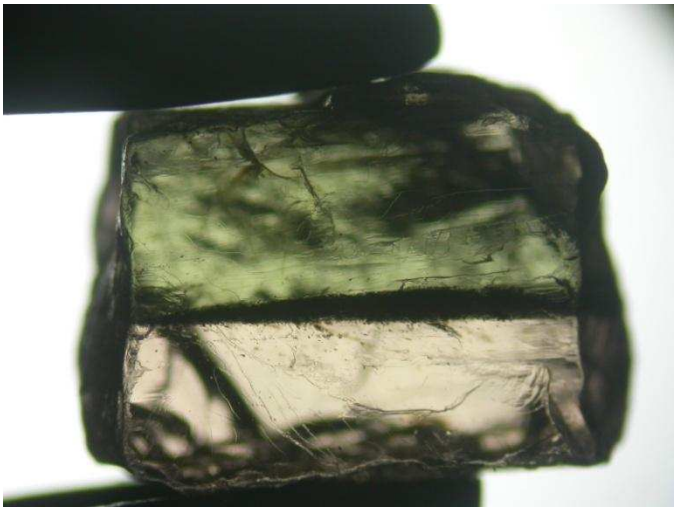

Figure 8: Many bicoloured samples of andalusite appeared to display various growth stages, with their colours separated by a sharp plane marked by brown granular inclusions. Magnified 25x

Specific Gravity. The samples had SG values in the 3.11–3.16 range. Webster (1994) listed SG values of 3.15–3.17, while Phillips and Griffen (1986) reported 3.13–3.16. The SG values of our samples are similar, though a few specimens had slightly lower values (probably due to fractures and surface-reaching inclusions).

Fluorescence. The samples were inert to long-wave UV radiation but fluoresced yellowish green to short-wave UV; the intensity varied from moderate to strong. Webster (1994) and O'Donoghue (2006) reported similar reactions for andalusite from Brazil.

Absorption Spectrum. With a desk-model spectroscope, a number of samples displayed a weak-to-strong diffuse band in the blue region at ~455 nm. When viewed along the c-axis, the absorption appeared weaker than in the perpendicular direction. Some samples did not exhibit any observable absorption.

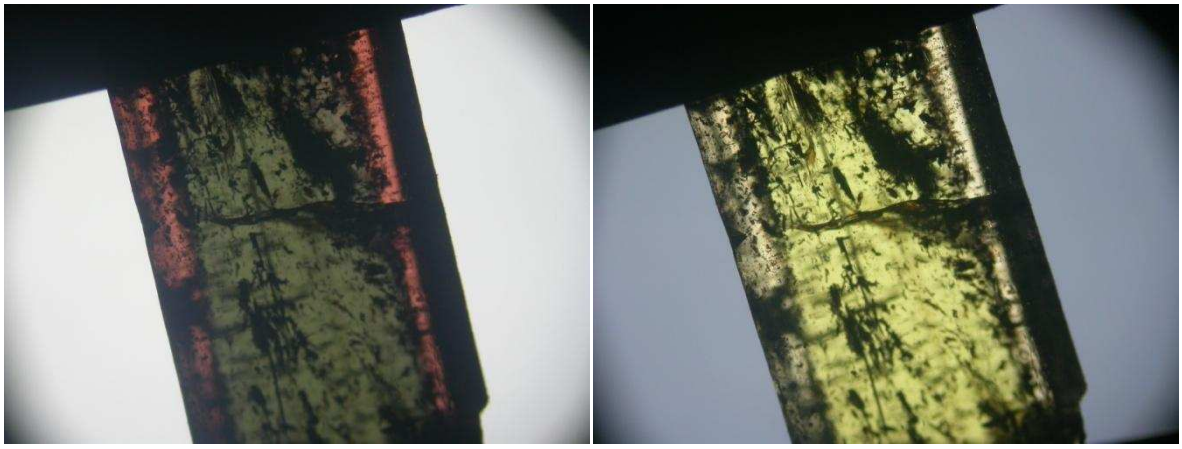

Figure 9: Many of the andalusite samples also exhibited colour zoning in green and brownish pink (left), a combination reminiscent of bicoloured tourmalines. When the polarizer was rotated 90°, the brownish pink area turned almost colourless, while the green portion became brighter yellowish green (right). Magnified 25x

TABLE 1: Properties of the Brazilian andalusite specimens studied.

Property	Description
Colour range	Green, yellowish green to brownish green, brownish pink, bicoloured green/pink, and pinkish brown (chiastolite)
Pleochroism	Brownish pink (parallel to the c-axis) Yellowish or brownish green (perpendicular to the c-axis)
Diaphaneity	Transparent to opaque
Refractive index / DR	n_α=1.637–1.649; n_γ=1.646–1.654; DR 0.008 - 0.010
Optic sign	Biaxial negative
Specific gravity	3.11–3.16
UV fluorescence	Inert (long-wave); Moderate to strong yellowish green (short-wave)
Absorption spectrum	Diffuse band at ~455 (weak to strong) in some samples
Microscopic features	Two types of curved inclusions, minute films/discs, numerous mineral inclusions, "fingerprints," pinpoints, twinning/growth patterns, cross patterns in chiastolite varieties
EDXRF analysis	Presence of Al, Si, Fe, Ca, and Cr (two specimens had Zn and Cu, probably due to contamination from the polishing wheels); no Mn detected in any samples
FTIR analysis	Complete absorption up to 2100 cm^{-1}; peaks at ~3687, 3652, and 3624 cm^{-1}; twin peaks at ~3520 and 3460 cm^{-1}; shoulders at ~3280 and 3095 cm^{-1}
Raman analysis	Several sharp peaks at ~1063, 917, 550, 463, 356, 325, and 290 cm^{-1}; smaller peaks at ~1120, 850, and 717 cm^{-1}

Microscopic Features. The samples displayed a wide range of internal patterns, such as curved features, mineral inclusions, and various twinning/growth patterns.

Curved Inclusion Features. Many samples contained numerous linear curved inclusions, of which two different varieties were defined: Type 1 inclusions occurred in the pleochroic brownish pink/green stones, while type 2 were present in some chiastolitic samples.

The type 1 curved inclusions were colourless and transparent, and had associated fine fringe-like films oriented perpendicular to their length (figure 10, left), giving the impression of icicles on branches. The cross sections of the inclusions appeared rectangular (figure 10, centre), and between crossed polarizers they were birefringent (figure 10, right), indicating their mineral nature. Gübelin and Koivula (2008) reported sillimanite fibres in andalusite from Santa Teresa in Minas Gerais, Brazil. The possibility of these tube-like inclusions being sillimanite cannot be ruled out, since their appearance seems consistent with the orthorhombic crystal form. Many of these inclusions also had a coating of some brownish epigenetic material where they reached the surface (again, see figure 10, left). EDXRF analysis of polished slices with these surface-reaching inclusions revealed the presence of Cu and Zn, which were absent from those without such surface-reaching inclusions. The Cu and Zn may have originated from the polishing wheels used, which contain these elements.

Figure 10: Type 1 curved inclusions were colourless and transparent, often with fine fringes (left and centre). They appeared birefringent between crossed polarizers, indicating their mineral nature (right). Note the stained surface and angle of curvature of these tubes, which are bent almost 90°. Magnified 40x (left), 80x (centre, brightfield illumination) and 70x (right, crossed polars).

The type 2 curved inclusions appeared to be growth tubes filled with a brown or black material. Some samples displayed these tubes in parallel bundles oriented in

various directions (figure 11, left). Each direction terminated at a sharp plane. In one specimen, these planes created a rectangular/square profile. They also appeared to run across the stone (similar to a twin plane) in different directions. At higher magnification, the tubes appeared to contain a black granular material (figure 11, right). Similar inclusions have been reported in "trapiche" tourmaline (Hainschwang et al., 2007), where growth channels are oriented in two directions. In our chiastolite specimens, the varying orientation of the growth tubes may be attributed to twinning or different stages of growth, as also indicated by the sharp growth zoning described below.

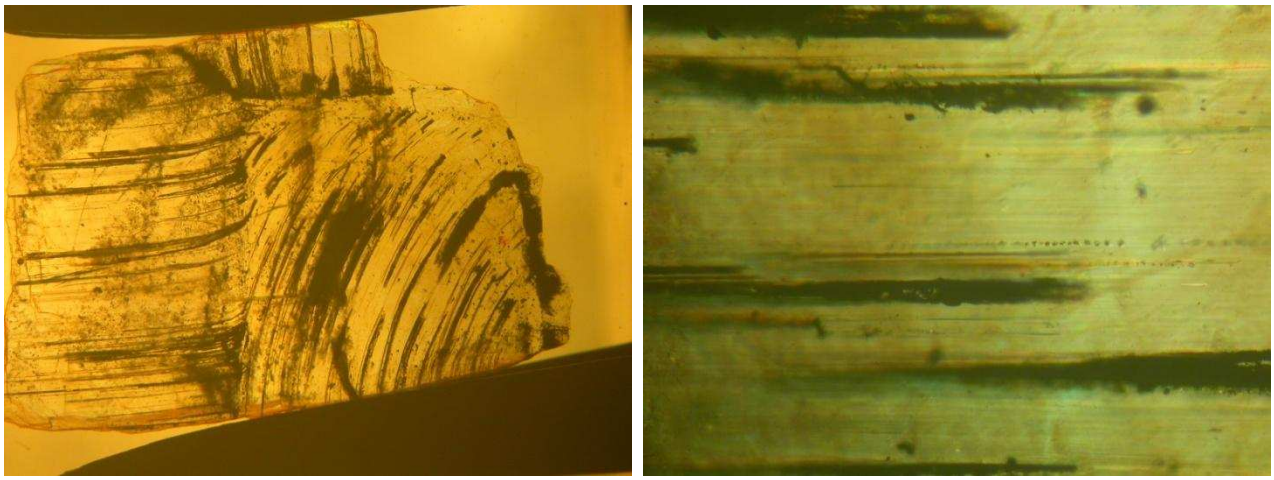

Figure 11: Type 2 curved inclusions consist of tubes that appear to be filled with a black material. In some samples, parallel groups of these tubes were oriented in various directions and delimited by sharp planes (left). At higher magnification, the black material appears to be granular (right). Magnified 30x (left, in immersion) and 80x (right).

The angle of curvature in both types of curved inclusions typically was almost 90^{o} (e.g., figure 10), while some appeared closer to 45^{o}, as if originating from pyramidal faces. Most of the inclusions were oriented parallel to the c-axis.

A few samples displayed an interesting pattern of type 2 tubes (figure 12). A central green core exhibited curved tubes parallel to the c-axis, while the surrounding portions contained tubes that radiated from the boundary with the core. The authors have previously observed a similar pattern of black tubes in chiastolites. Such a growth pattern indicates different growth stages and directions of the overgrown areas and is a characteristic of chiastolite.

In addition to the curved tubes, we observed straight tubes with slightly wavy surfaces (figure 13), again oriented parallel to the c-axis. These were mainly in the yellow-green and bicoloured samples, and as well as in chiastolites with green cores.

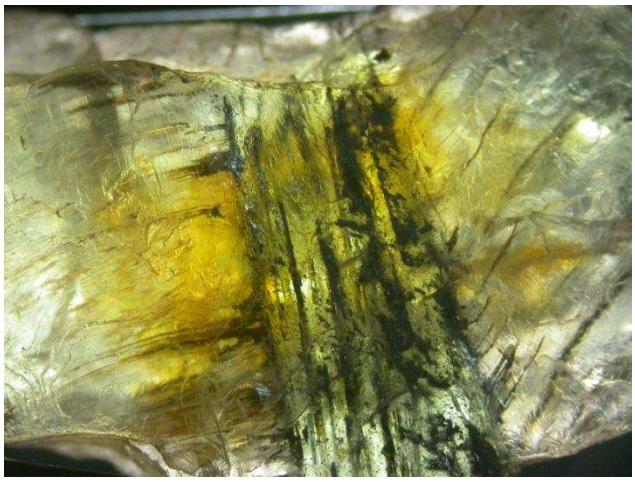

Figure 12: In a few chiastolite specimens, a green core contained tubes oriented parallel to the c-axis, while the surrounding area hosted tubes in a radiating pattern. Similar patterns of black tubes have been observed previously in chiastolite by the authors. Magnified 25x

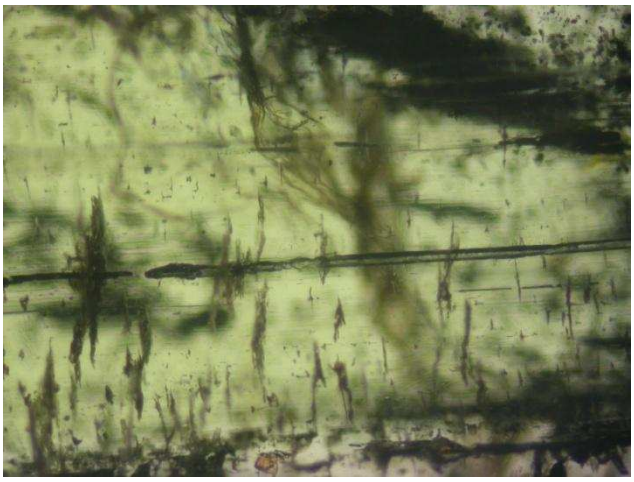

Figure 13: Straight tubes with wavy surfaces, oriented parallel to the c-axis, were present in some of the andalusite samples. Magnified 60x

Films and Discs. Many of the samples had rows of small films or discs oriented along the c-axis in a "stringer"-like pattern (figure 14) similar to the "fringes" associated with the type 1 curved inclusions discussed above. In one of the samples, some films were associated with small conical tube-like features that resembled nail-head spicules (figure 15). These films were oriented roughly along the basal plane, while the conical tubes were oriented along the c-axis. Although nail-head spicules are commonly associated with synthetic gems grown by hydrothermal or flux processes, they have also been reported in a few natural stones such as sapphire and emerald (Choudhary and Golecha, 2007).

Figure 14: The andalusites commonly contained film or platelet-like inclusions that appeared to be oriented along the c-axis (vertical in this view), giving a stringer-like pattern as in figure 10 (left). Magnified 65x

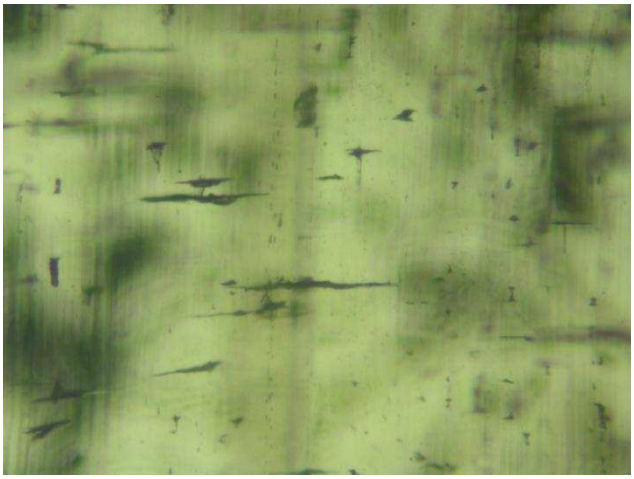

Figure 15. In one sample, small films/fractures were associated in places with conical tube-like features (similar to nail-head spicules). These films were oriented roughly along the basal plane (horizontal in this view), while the conical "tubes" were along the c-axis. Also note the growth zoning parallel to the c-axis. In addition, many scattered tiny inclusions were visible that could not be resolved clearly. Magnified 80x

Mineral Inclusions. The cross pattern of black granular inclusions in chiastolite is the result of rapid growth of the prism faces, which pushed the black material to the edges. Although we did not analyze them for this study, similar black inclusions in chiastolite have been identified as graphite (Johnson and Koivula, 1998; Hlaing, 2000). Scattered colourless to brown and black crystals (figure 16) were also present. Many of these crystal inclusions were elongated and birefringent between crossed polarizers, and some displayed cleavage-like planes oriented perpendicular to their length. They were confined to two directional planes intersecting at 90^{o} to form a square or rectangular outline. This orientation indicated that different growth sectors were separated by these crystal inclusions. This inclusion pattern has not been reported previously for chiastolite. However, such features are not expected in a faceted andalusite since a cutter would surely exclude them.

Also seen were brownish birefringent platelets oriented in planes. In the green and brownish pink varieties they appeared scattered, while they were more defined (i.e., along the planes of the core) in the chiastolitic material.

Fingerprints. A few stones had "fingerprint" inclusions forming a crisscross veil-like pattern (figure 17). These appeared to be composed of crystals rather than fluid, judging from the sharp edges of the individual inclusions.

Pinpoints. We observed whitish pinpoints in a few samples. These pinpoints were restricted to straight, wavy, and curved zones (figure 18) that appeared white and were oriented parallel to the c-axis.

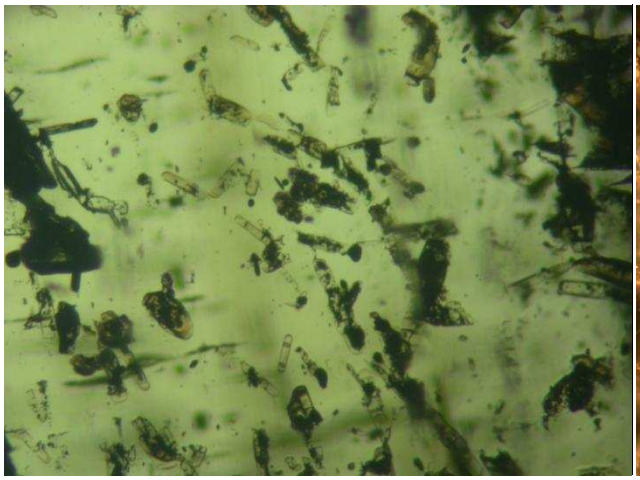

Figure 16: Scattered crystalline inclusions were present in the andalusites. Some of these inclusions were birefringent between crossed polarizers. Magnified 80x

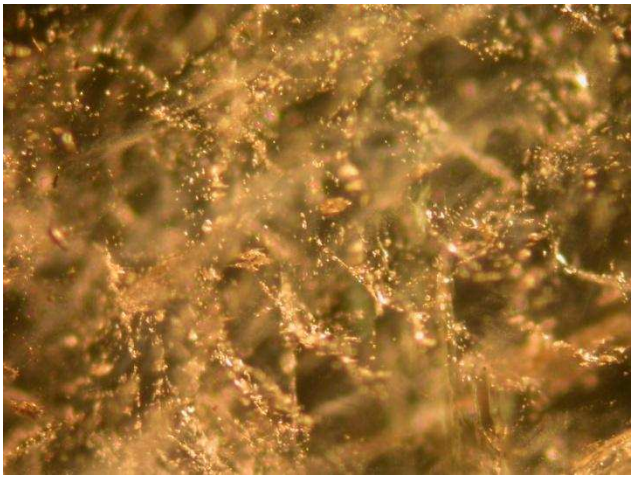

Figure 17: A few andalusite samples displayed veil-like "fingerprints" that appeared to be composed of crystals. Magnified 60x

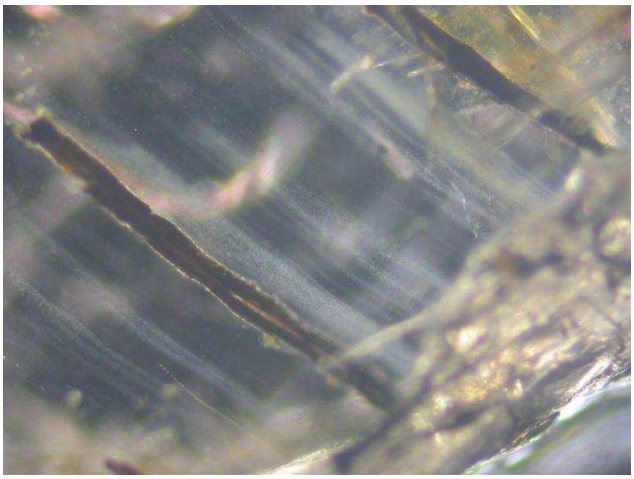

Figure 18: Fine whitish pinpoints arranged in straight, curved, or wavy zones were observed in a few andalusite samples. Magnified 65x

Growth Features. The study samples displayed a wide range of growth features, some of which were quite complex. Many exhibited distinct colour zones when viewed with the unaided eye, and also revealed unusual and interesting patterns with magnification. In one case, two colours—green and light pink—were clearly separated by a brown zone. With magnification, this zone appeared to be composed of tiny crystals (as they appear granular; see figure 8). In a few specimens, distinct brownish pink and green zones were separated by sharp planes, often containing some mineral inclusions (again, see figure 9, left). This suggests two stages of growth with different chemical compositions, as is the case for colour-zoned sapphire or bicoloured tourmaline; both colour components also displayed a strong degree of pleochroism (again, see figure 9). Such bicoloured andalusite specimens, when viewed along the c-axis, had the central green core and light brownish pink to red to almost colourless outer layers following the crystal shape with a square-to-rectangular profile similar to that illustrated in figure 7.

Many samples also displayed growth zones that were oriented parallel to the prism face or the c-axis (again, see figure 15). Some of the chiastolite samples also exhibited "wavy" alternating yellow and brown colour and growth zones.

EDXRF Analysis. Qualitative EDXRF analysis was performed on polished samples as well as preforms. Stones were oriented to analyze both brownish pink and green areas to check for variations in chemical composition; this included colour-zoned samples as well as those of different homogeneous bodycolours. However, no chemical variations were observed. The analyses revealed the presence of Al and Si, as expected for andalusite. A minor amount of Fe was also detected, along with traces of Ca and Cr. Manganese was not detected in any of the samples, consistent with the low birefringence and the RI values.

FTIR Spectroscopy. The FTIR spectra displayed complete absorption below 2100 cm^{-1} and a number of bands of varying intensity in the 3800–3000 cm^{-1} region (figure 19): three at ~3687, 3652, and 3624 cm^{-1} in most samples; a pair at about 3520 and 3460 cm^{-1} in

almost all samples; two bands at ~3280 and 3095 cm^{-1} in most samples; and weak features at ~3380 and 3170 cm^{-1}.

All the features recorded in this study are in the water region of the IR spectrum and correspond to vibrations and stretching of OH molecules (Busigny et al., 2004; Balan et al., 2006). Although andalusite is considered an anhydrous mineral, this suggests the presence of some water (H_2O or OH), either in the structure or in inclusions. Peaks at 3520 and 3460 cm^{-1} suggest that OH dipoles lie within the {001} basal plane of andalusite (Burt et al., 2006); these two peaks appeared much stronger when the spectra were collected along the c-axis or in the brownish pink colour direction.

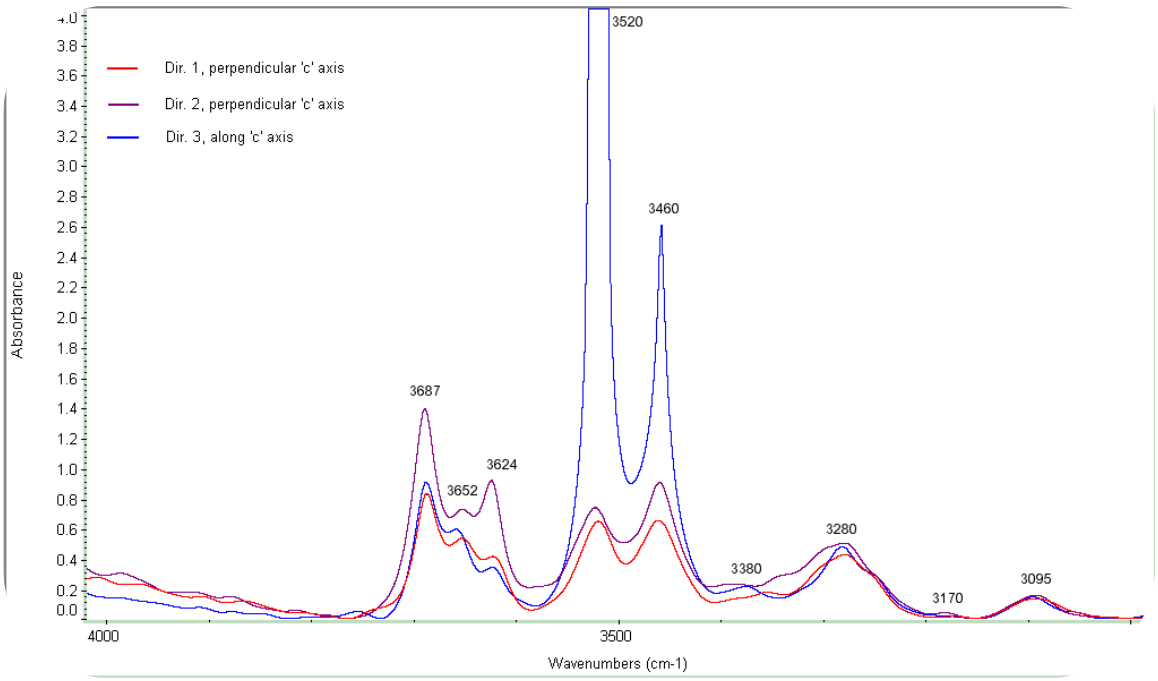

Figure 19: The infrared absorption spectra revealed a number of weak-to-strong peaks in the 3800–3000 cm^{-1} region in both pleochroic directions. The peaks at 3520 and 3460 cm^{-1}, were much stronger in the brownish pink direction, suggesting the presence of OH dipoles in the basal plane.

Raman Analysis. No directional variations were recorded in the Raman spectra. There were several sharp peaks at ~1063, 917, 550, 463, 356, 325, and 290 cm^{-1}, with smaller peaks at ~1120, 850, and 717 cm^{-1}. The spectral pattern is similar to those reported for andalusites in the RRUFF project database (www.rruff.info). Peaks in the 1150–800 cm^{-1} region arise from Si-O stretching, while those below 600 cm^{-1} are due to complex

motions between O, OH, and SiO_4 (Wang et al., 2002), suggesting the presence of OH in the structure of the andalusite.

Treatment Experiments. Heat treatment at 350°C and 550°C yielded no noticeable change in colour; heating at 800°C resulted in only a subtle lightening of the bodycolour, though it has been reported previously that "olive" green andalusite from Brazil changes to pink and brown, and then to colourless, at 800°C (Nassau, 1994).

Microscopic examination of the samples heated at the lower temperatures did not reveal any observable effects. In the samples that were heated to 800°C, however, some changes were observed, though they were not distinct enough to be considered diagnostic evidence of heating. These samples developed some stress fractures oriented in one direction along the prism faces, indicating the expansion of cleavage planes due to heat. Samples containing tube-like inclusions with brownish material also displayed some changes; the brown material burst from within the tubes and concentrated in associated fractures, thereby giving the effect of iron-stained films or fractures. Some samples also developed similar patches or films on the surface, possibly resulting from the oxidation of Fe in the structure of andalusite.

The three specimens subjected to fracture filling with resin showed an obvious improvement in apparent clarity, while the two filled with oil displayed only a minute change in the visibility of inclusions. The resin filling was detectable in the infrared spectra, which displayed a characteristic band at 3046 cm^{-1} as well as peaks at 2926 and 2854 cm^{-1}. The latter bands are associated with oils and epoxy prepolymers (Johnson et al., 1999). The stones filled with oil also displayed the characteristic 2926 and 2854 cm^{-1} bands.

Conclusion

The colour range of the Brazilian andalusite study samples varied from yellowish green to green to brownish pink, with some bicoloured green and brownish pink. The transparent chiastolite samples were quite unusual for this gem variety. Gemmological properties such as RI and SG, along with a characteristically strong pleochroism, easily distinguish

andalusite from other gems such as tourmaline (which has weaker pleochroism and is uniaxial). EDXRF analysis revealed the presence of Fe, Ca, and Cr, in addition to Al and Si; no Mn was detected in any of the samples, consistent with the low RI and birefringence values. In addition to these properties, FTIR and Raman analysis revealed peaks in the 3800–3000 cm^{-1} and 1100–200 cm^{-1} regions, respectively. These features indicated vibrations or stretching of OH and SiO_4 molecules in this primarily anhydrous mineral. The most unusual findings of the inclusion study were the curved inclusions seen in many of the samples and the growth patterns associated with the bicoloured stones.

References

Balan E., Lazzeri M., Mauri F. (2006) Infrared spectrum of hydrous minerals from first-principles calculations. *Ab Initio (from Electronic Structure) Calculation of Complex Processes in Materials*, Ψ_k Newsletter No. 75, June 2006, pp. 143–150, www.psi-k.org/newsletters/News_75/newsletter_75.pdf [date accessed January 3, 2009].

Burt J.B., Ross N.L., Gibbs G.V., Rossman G.R., Rosso K.M. (2007) Potential protonation sites in the Al2SiO5 polymorphs based on polarized FTIR spectroscopy and bond critical point properties. Physics and Chemistry of Minerals, Vol. 34, pp. 295–306.

Busigny V., Cartigny P., Philipot P., Javoy M. (2004) Quantitative analysis of ammonium in biotite using infrared spectroscopy. *American Mineralogist*, Vol. 89, pp. 1625–1630.

Choudhary G., Golecha C. (2007) A study of nail-head spicule inclusions in natural gemstones. *Gems & Gemology*, Vol. 43, No. 3, pp. 228–235.

Dana E.S., Ford W.E. (1992) *A Textbook of Mineralogy with an Extended Treatise on Crystallography and Physical Mineralogy*, 4th ed. Wiley Eastern Ltd., New Delhi, India.

Gribble C.D. (1991) *Rutley's Elements of Mineralogy*, 27th ed., 1st Indian reprint. CBS Publishers & Distributors, Delhi, India.

Gübelin E.J., Koivula J.I. (2008) *Photoatlas of Inclusions in Gemstones*, Vol. 2. Opinio Publishers, Basel, Switzerland.

Hainschwang T., Notari F., Anckar B. (2007) Trapiche tourmaline from Zambia. *Gems & Gemology*, Vol. 43, No. 1, pp. 36–46.

Hlaing T. (2000) Chiastolite from Kyaukse, Myanmar. *Australian Gemmologist*, Vol. 20, No. 11, pp. 479–480.

Hora Z.D. (1997) Andalusite hornfels, in *Geological Fieldwork 1997*. British Columbia Ministry of Employment and Investment, Paper 1998-1, pp. 24N-1–24N-3.

Johnson M.L., Koivula J.I., Eds. (1998) Gem News: Andalusite (chiastolite) sphere. *Gems & Gemology*, Vol. 34, No. 1, p. 51.

Johnson M.L., Elen S., Muhlmeister S. (1999) On the identification of various emerald filling substances. *Gems & Gemology*, Vol. 35, No. 2, pp. 82–107.

Kerr P.F. (1959) *Optical Mineralogy*. McGraw-Hill Book Co., London.

Liu G. (2006) *Fine Minerals of China: A Guide to Mineral Localities*. AAA Minerals AG, Zug, Switzerland.

Nassau K. (1994) *Gemstone Enhancement: History, Science and State of the Art*, 2nd ed. Butterworth-Heinemann, Oxford, UK.

O'Donoghue M., Ed. (2006) *Gems*, 6th ed. Butterworth-Heinemann, Oxford, UK.

Phillips W.M., Griffen D.T. (1986) *Optical Mineralogy: The Nonopaque Minerals*, 1st Indian ed. CBS Publishers & Distributors, New Delhi, India.

Putnis A. (1992) *Introduction to Mineral Sciences*. Cambridge University Press, Cambridge, UK.

Roberts W.L., Campbell T.J., Rapp G.R. (1990) *Encyclopedia of Minerals*, 2nd ed. Van Nostrand Reinhold Co., New York.

Wang A., Freeman J., Kuebler K.E. (2002) Raman spectroscopic characterization of phyllosilicates, *Lunar and Planetary Science XXXIII*, www.lpi.usra.edu/meetings/lpsc2002/pdf/1374.pdf [date accessed January 12, 2009]

Webster R. (1994) *Gems: Their Sources, Descriptions, and Identification*, 5th ed. Revised by P.G. Read, Butterworth-Heinemann, Oxford, UK.

Acknowledgments

The authors are grateful to Frank Fernandes of M/s. Neethi's in Jaipur for loaning, the samples for study, some of which he also cut and polished, as well as for helpful discussions on determining the refractive index variations according to crystal orientation. The authors also express their gratitude to the Indian Institute of Jewellery in Mumbai for collecting Raman spectra at their facility.

All photographs and photomicrographs by Gagan Choudhary